SOFT SCATTERING AT LHC ENERGIES

Errol Gotsman
Tel Aviv University

(work done with Genya Levin and Uri Maor)

Outline

- The measurement of the pp total cross-section by the TOTEM collaboration at W $=$ 7 TeV ($\sigma_{tot} = 98.3 \pm 0.2^{stat} \pm 2.8^{syst}$) caused an "upheaval", since most models which prior to this were successful in describing "soft" p-p and $\bar{p}$-p interactions at energies $\leq$ 1.8 TeV, predicted a lower result.
- IS THERE A CHANGE IN THE BEHAVIOUR OF σ_{tot} FOR W $>$ 1.8 TEV?
- The dilemma facing the different groups was:

  A) Does one just attempt to change the POMERON'S parameters ?

  OR

  B) Does one make a comprehensive revision of the underlying structure of POMERON models, for high energy soft interactions ?
- GLM chose path A) , some other groups chose B)
  I will discuss our revised parametrization, and compare with the approach and results of other models on the market.

Good-Walker Formalism

The Good-Walker (G-W) formalism, considers the diffractively produced hadrons as a single hadronic state described by the wave function Ψ_D, which is orthonormal to the wave function Ψ_h of the incoming hadron (proton in the case of interest) i.e. $< \Psi_h | \Psi_D >= 0$.

One introduces two wave functions ψ_1 and ψ_2 that diagonalize the 2x2 interaction matrix $\mathbf{T}$

$$A_{i,k} =< \psi_i \, \psi_k | \mathbf{T} | \psi_{i'} \, \psi_{k'} >= A_{i,k} \, \delta_{i,i'} \, \delta_{k,k'}.$$

In this representation the observed states are written in the form

$$\psi_h = \alpha \, \psi_1 + \beta \, \psi_2 \, ,$$
$$\psi_D = -\beta \, \psi_1 + \alpha \, \psi_2$$

where, $\alpha^2 + \beta^2 = 1$

Good-Walker Formalism-2

The s-channel Unitarity constraints for (i,k) are analogous to the single channel equation:

$$Im\, A_{i,k}\,(s,b) = |A_{i,k}\,(s,b)\,|^2 + G^{in}_{i,k}(s,b),$$

$G^{in}_{i,k}$ is the summed probability for all non-G-W inelastic processes, including non-G-W "high mass diffraction" induced by multi-$I\!P$ interactions. A simple solution to the above equation is:

$$A_{i,k}(s,b) = i\left(1 - \exp\left(-\frac{\Omega_{i,k}(s,b)}{2}\right)\right), G^{in}_{i,k}(s,b) = 1 - \exp\left(-\Omega_{i,k}(s,b)\right).$$

The opacities $\Omega_{i,k}$ are real, determined by the Born input.

Good-Walker Formalism-3

Amplitudes in two channel formalism are:

$$a_{el}(s,b) = i\{\alpha^4 A_{1,1} + 2\alpha^2\beta^2 A_{1,2} + \beta^4 A_{2,2}\},$$

$$a_{sd}(s,b) = i\alpha\beta\{-\alpha^2 A_{1,1} + (\alpha^2 - \beta^2)A_{1,2} + \beta^2 A_{2,2}\},$$

$$a_{dd}(s,b) = i\alpha^2\beta^2\{A_{1,1} - 2A_{1,2} + A_{2,2}\}.$$

With the G-W mechanism σ_{el} , σ_{sd} and σ_{dd} occur due to elastic scattering of ψ_1 and ψ_2, the correct degrees of freedom.

Examples of Pomeron diagrams

leading to diffraction NOT included in G-W mechanism

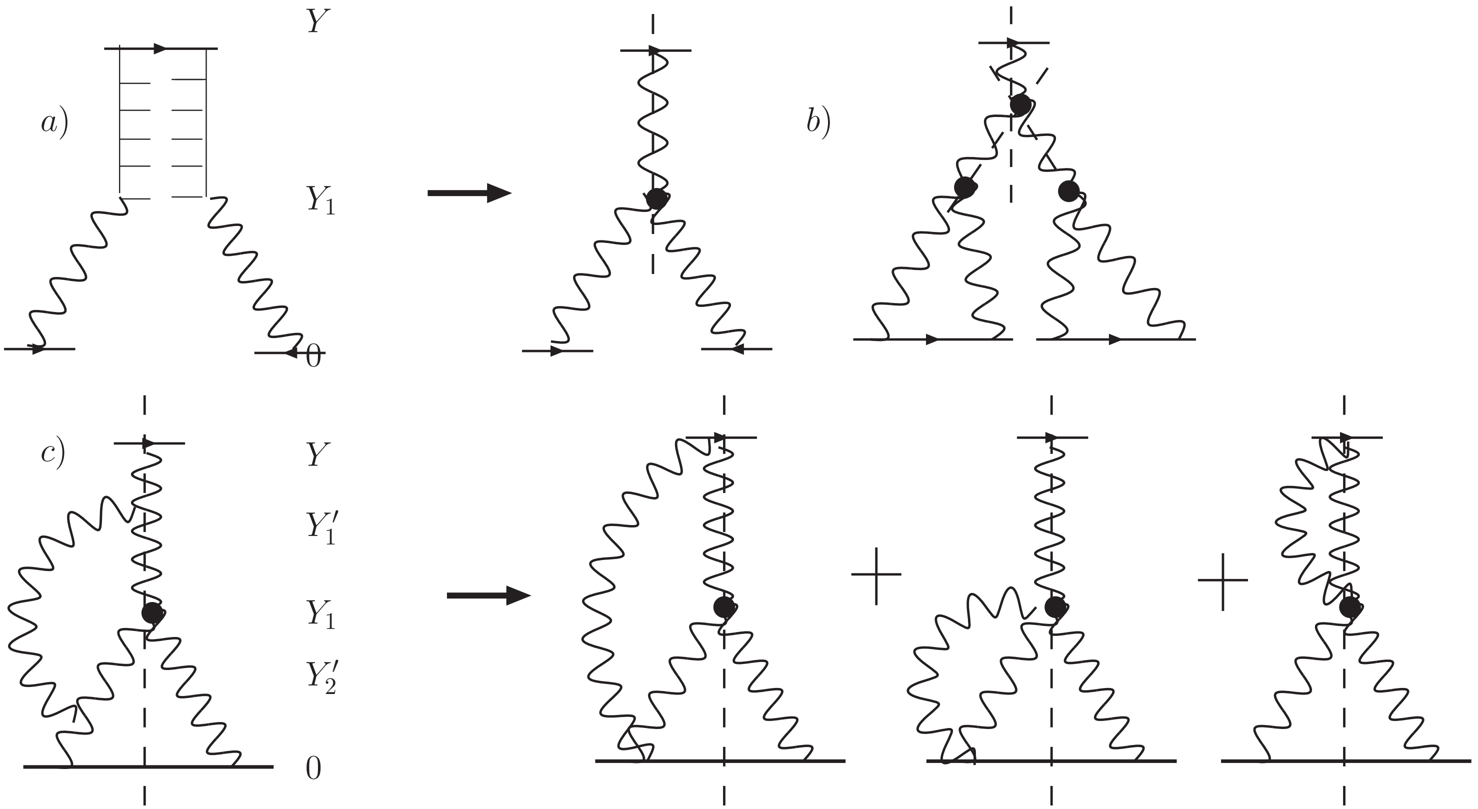

Examples of the Pomeron diagrams that lead to a different source of the diffractive dissociation that cannot be described in the framework of the G-W mechanism. (a) is the simplest diagram that describes the process of diffraction in the region of large mass $Y - Y_1 = \ln(M^2/s_0)$. (b) and (c) are examples of more complicated diagrams in the region of large mass. The dashed line shows the cut Pomeron, which describes the production of hadrons.

Example of enhanced and semi-enhanced diagram

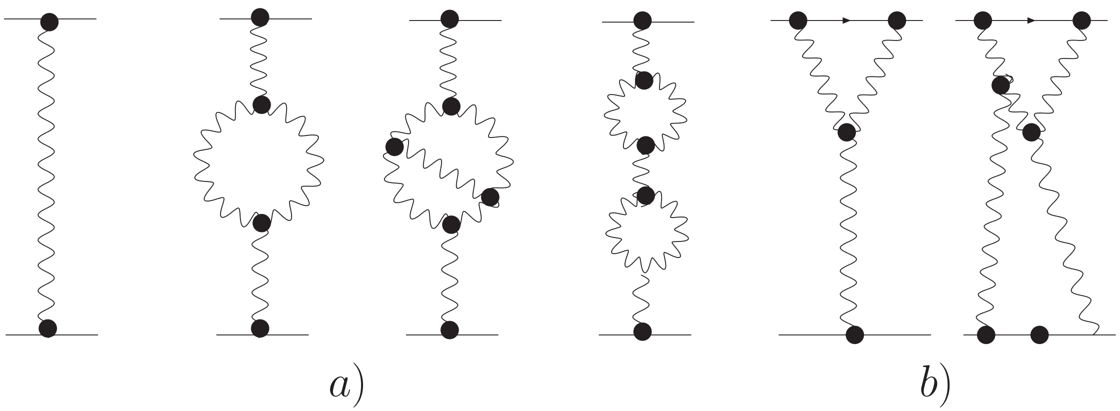

Different contributions to the Pomeron Green's function
a) examples of enhanced diagrams ;
(occur in the renormalisation of the Pomeron propagator)
b) examples of semi-enhanced diagrams
(occur in the renormalisation of the $I\!\!P$ -p vertex)
Multi-Pomeron interactions are crucial for the production of LARGE MASS DIFFRACTION

Our Formalism 1

The input opacity $\Omega_{i,k}(s,b)$ corresponds to an exchange of a single bare Pomeron.

$$\Omega_{i,k}(s,b) \;=\; g_i(b)\, g_k(b)\, P(s).$$

$P(s) \;=\; s^{\Delta}$ and $g_i(b)$ is the Pomeron-hadron vertex parameterized in the form:

$$g_i\,(b) \;=\; g_i\, S_i(b) \;=\; \frac{g_i}{4\pi}\, m_i^3\, b\, K_1\,(m_i b)\,.$$

$S_i(b)$ is the Fourier transform of $\frac{1}{(1+q^2/m_i^2)^2}$, where, q is the transverse momentum carried by the Pomeron.

The Pomeron's Green function that includes all enhanced diagrams is approximated using the MPSI procedure, in which a multi Pomeron interaction (taking into account only triple Pomeron vertices) is approximated by large Pomeron loops of rapidity size of $\ln s$. The Pomeron's Green Function is given by

$$G_{I\!P}\,(Y) \;=\; 1 \;-\; \exp\left(\frac{1}{T\,(Y)}\right) \frac{1}{T\,(Y)}\,\Gamma\left(0, \frac{1}{T\,(Y)}\right),$$

where $T\,(Y) \;=\; \gamma\, e^{\Delta_{I\!P} Y}$ and $\Gamma\,(0, 1/T)$ is the incomplete gamma function.

Our Formalism 2

Summing the net diagrams , we replace $g_i(b)$ by a more complicated vertex function which, together with the enhanced diagrams, results in the following expression for $\Omega_{i,k}(s,b)$:

$$\Omega^{i,k}_{I\!P}(Y;b) \;=\; \int d^2b' \; \frac{g_i\left(\vec{b}'\right)\, g_k\left(\vec{b}-\vec{b}'\right)\, \left(1/\gamma\, G_{I\!P}\,(T(Y))\right)}{1 + (G_{3I\!P}/\gamma)\, G_{I\!P}\Big(T(Y)\Big)\, \left[g_i\left(\vec{b}'\right) + g_k\left(\vec{b}-\vec{b}'\right)\right]}.$$

$G_{3I\!P}$ is the triple Pomeron vertex

and $\gamma =$ low energy amplitude of the dipole-target interaction

Our Formalism 3: Diffractive Processes

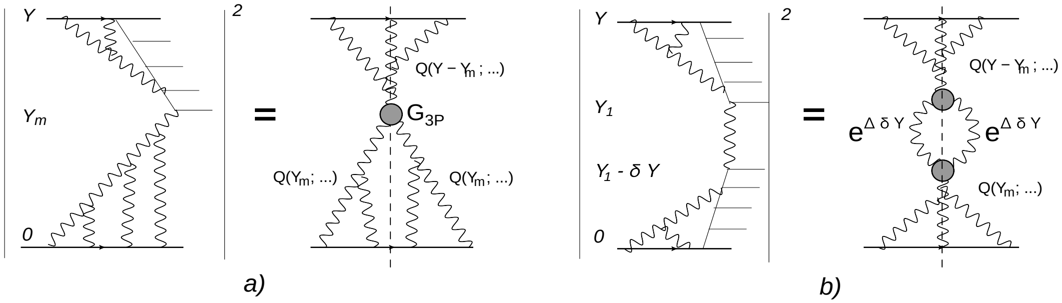

For diffraction production we introduce an additional contribution due to the Pomeron enhanced mechanism which is non GW.

As shown in fig-a, for (single diffraction) we have one cut Pomeron,

and in fig-b, for (double diffraction) we have two cut Pomerons

we express the cut Pomerons through a Pomeron without a cut, using the AGK cutting rules.

Fits GLM1 and GLM2

GLM1 [EPJ C71,1553 (2011)]

The parameters of GLM1 (prior to LHC) were determined by fitting to data $20 \leq W \leq 1800$ GeV.

We had 58 data points and obtained a $\chi^2/d.f. \approx 0.86$.

This fit yields a value of $\sigma_{tot} = 91.2$ mb at W = 7 TeV.

Problem is that most data is at lower energies (W $\leq$ 500 GeV) and these have small errors, and hence have a dominant influence on the determination of the parameters.

GLM2 [Phys.Rev. D85, 094007 (2012)]

To circumvent this we made a new fit GLM2 to data for energies W $>$ 500 GeV (including LHC), to determine the Pomeron parameters. We included 35 data points.

We then tuned the values of the Pomeron-proton vertex and the $G_{3\mathbb{P}}$ coupling, to give smooth cross sections over the complete energy range $20 \leq W \leq 7000$ GeV.

Values of Fit Parameters for GLM2 and (GLM1)

$\Delta_{I\!P}$	β	$\alpha'_{I\!P}(GeV^{-2})$	$g_1\,(GeV^{-1})$	$g_2\,(GeV^{-})$	m_1 (GeV)	m_2 (GeV)
0.21(0.2)	0.46(0.388)	0.028(0.02)	1.89(2.53)	61.99(88.87)	5.045(2.648)	1.71(1.37)
$\Delta_{I\!R}$	γ	$\alpha'_{I\!R}\,(GeV^{-2})$	$g_1^{I\!R}\,(GeV^{-1})$	$g_2^{I\!R}\,(GeV^{-1})$	$R^2_{0,1}\,(GeV^{-1})$	$G_{3I\!P}\,(GeV$
- 0.47(-0.466)	0.0045(0.0033)	0.4(0.4)	13.5(14.5)	800(1343)	4.0(4.0)	0.03(0.0173)

- $g_1(b)$ and $g_2(b)$ describe the vertices of interaction of the Pomeron with state 1 and state 2
- The Pomeron trajectory is $1 + \Delta_{I\!P} + \alpha^{'}_{I\!P}$t
- γ denotes the low energy amplitude of the dipole-target interaction
- β denotes the mixing angle between the wave functions
- $G_{3I\!P}$ denotes the triple Pomeron coupling

Comparison of the Impact Parameter Dependence of GLM Amplitudes

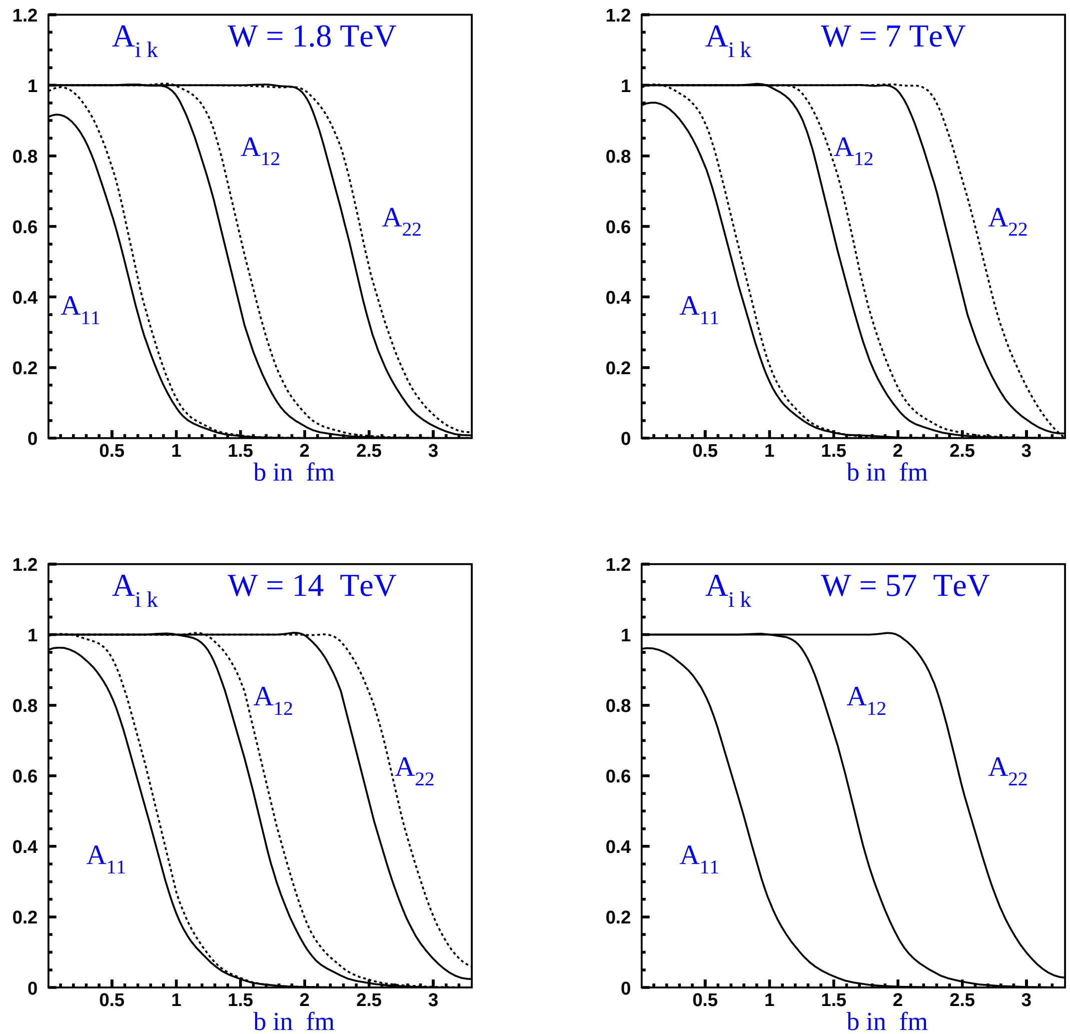

The solid lines are associated with GLM2 while the dotted lines with GLM1

Comparison of Results of GLM1 and GLM2

$\sqrt{s}$ TeV	1.8	7	8
σ_{tot} mb	75.6 (74.4)	94.2 (91.3)	96.1
σ_{el} mb	18.2 (17.5)	22.9 (23)	23.5
$\sigma_{sd}(M \leq M_0)$ mb		$10.5 + (2.6)^{nGW}$ (10.2)	$10.6 + (2.64)^{nGW}$
$\sigma_{sd}(M^2 < 0.05s) mb$	$8.97 + (1.95)^{nGW}$ (8.87)	$10.5 + (3.94)^{nGW}$ (10.2)	$10.6 + (4.04)^{nGW}$
σ_{dd} mb	$5.56 + (0.369)^{nGW}$ (4.46)	$5.98 + (1.166)^{nGW}$ (6.46)	$6.08 + (1.2)^{nGW}$
$B_{el}\ GeV^{-2}$	17.6 (16.1)	19.8 (19.3)	20.0
$B^{GW}_{sd}\ GeV^{-2}$	6.36	8.01	8.15
σ_{inel} mb	57.4	71.7	72.6

$\sqrt{s}$ TeV	14	57	100
σ_{tot} mb	104.0(101.)	125.0	134.0
σ_{el} mb	26.1(26.1)	32.8	35.5
$\sigma_{sd}(M^2 < 0.05s)$ mb	$11.2 + (5.58)^{nGW}$(10.8)	$12.8 + (8.19)^{nGW}$	13.4 ++
σ_{dd} mb	$6.55 + (1.5)^{nGW}$(6.65)	$7.68 + (4.9)^{nGW}$	8.13 +
$B_{el}\ GeV^{-2}$	21.2(20.5)	24.1	25.3
σ_{inel} mb	77.9	92.9	98.5

Predictions of our model for different energies W. M_0 is taken to be equal to $200GeV$ as ALICE measured the cross section of the diffraction production with this restriction.

Comparison of the predictions of GLM2 and LHC data at 7 TeV

W	σ_{tot}^{model}(mb)	σ_{tot}^{exp}(mb)	σ_{el}^{model}(mb)	σ_{el}^{exp}(mb)
7 TeV	94.2	TOTEM: 98.3 $\pm 0.2^{st}$ $\pm 2.8^{syst}$	22.9	TOTEM: 24.8$\pm 0.2^{st} \pm 1.2^{syst}$

W	$\sigma_{in}^{model}(mb)$	σ_{in}^{exp}(mb)	$B_{el}^{model}(GeV^{-2})$	$B_{el}^{exp}(GeV^{-2})$
7 TeV	71.7	CMS: 68.0$\pm 2^{syst} \pm 2.2^{lumi} \pm 4^{extrap}$ ATLAS: 69.4$\pm 2.4^{exp} \pm 6.9^{extrap}$ ALICE: 72.7 $\pm 1.1^{model} \pm 5.1^{extrap}$ TOTEM: 73.5 $\pm 0.6^{st} \pm 1.8^{syst}$	19.8	TOTEM: 20.1$\pm 0.2^{st} \pm 0.3^{s}$

W	$\sigma_{sd}^{model}(mb)$	σ_{sd}^{exp}(mb)	σ_{dd}^{model}(mb)	σ_{dd}^{exp}(mb)
7 TeV	$10.5^{GW} + 2.6^{nGW}$	ALICE : 14.16 $\pm$ 3	$5.98^{GW} + 1.166^{nGW}$	ALICE: 8.86 $\pm$ 3

Comparison of the Energy Dependence of GLM2 and Experimental Data

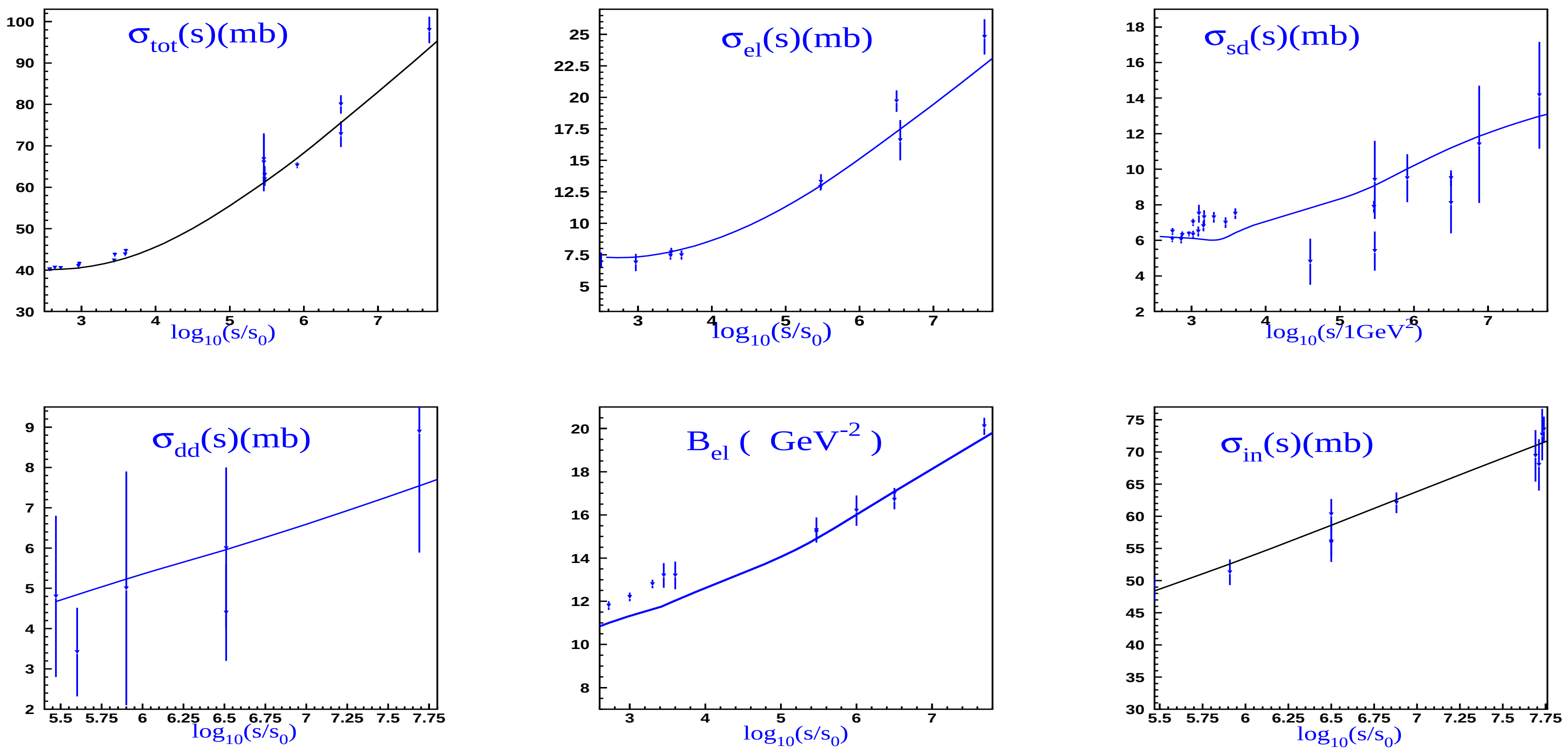

From Donnachie and Landshoff arXiv:1112.2485

D and L use an eikonalized Regge pole model with Pomerons and Reggeons:

The values of the parameters are determined by making a simultaneous fit to pp scattering data and to DIS lepton scattering for low x.

Their results can be summarized:

	SOFT POMERON	HARD POMERON
	$\alpha_S^{I\!P} = 1.093 + 0.25t$	$\alpha_H^{I\!P} = 1.362 + 0.1t$
Coupling strength:	$X_1 = 243.5$	$X_0 = 1.2$
At 7 TeV	$\sigma_{tot}(\text{soft}) = 91$ mb	$\sigma_{tot}(\text{hard} + \text{soft}) = 98$ mb

From Donnachie and Landshoff arXiv:1112.2485

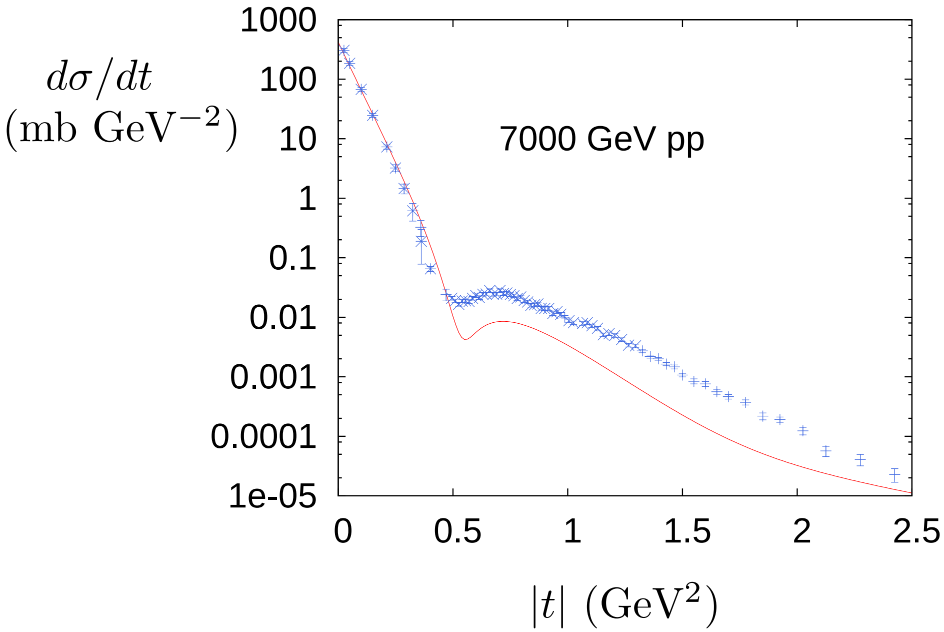

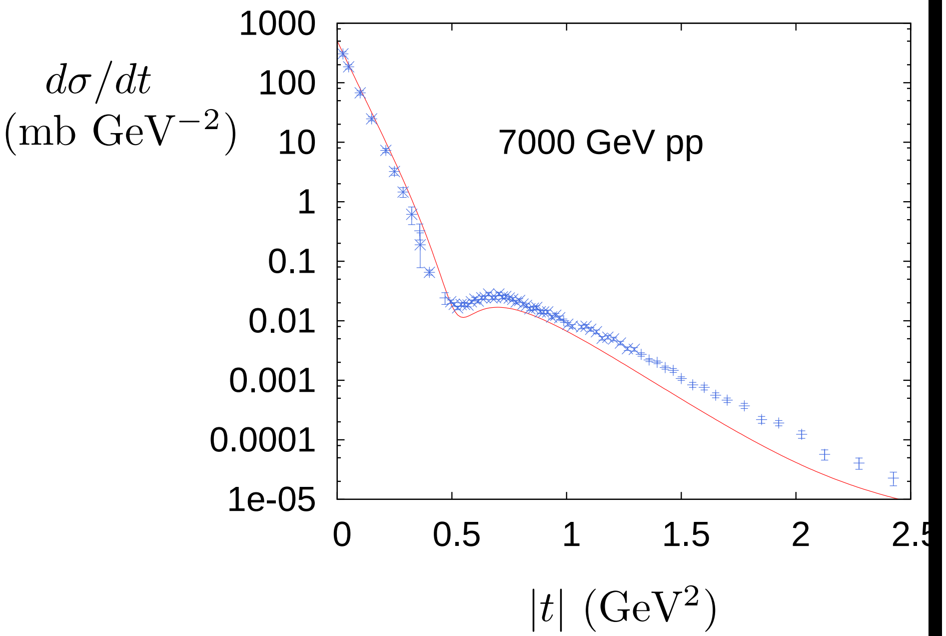

NO HARD POMERON

(HARD + SOFT) POMERON

From Ciesielski and Goulianos "MBR MC Simulation" arXiv:1205.1446

The $\sigma_{\rm tot}^{p^{\pm}p}(s)$ cross sections at a pp center-of-mass-energy $\sqrt{s}$ are calculated as follows:

$$\sigma_{\rm tot}^{p^{\pm}p} = \begin{cases} 16.79 s^{0.104} + 60.81 s^{-0.32} \mp 31.68 s^{-0.54} & \text{for } \sqrt{s} < 1.8 \text{ TeV}, \\ \sigma_{\rm tot}^{\rm CDF} + \frac{\pi}{s_0}\left[\left(\ln\frac{s}{s_F}\right)^2 - \left(\ln\frac{s^{\rm CDF}}{s_F}\right)^2\right] & \text{for } \sqrt{s} \geq 1.8 \text{ TeV}, \end{cases}$$

The energy at which "saturation " occurs $\sqrt{s_F} = 22$ GeV, and $s_0 \,=\, 3.7 \pm 1.5\, GeV^2$.

Block and Halzen's Parametrization of σ_{tot} and σ_{inel}

Bloch and Halzen (P.R.L. 107,212002 (2011) and arXiv:1205.5514) claim that the experimental data from LHC (at 7 Tev) and Auger (at 57 Tev), "saturate" the Froissart bound of $ln^2 s$. By "saturation" they mean that $\sigma_{tot} \approx ln^2 s$.

Using Analyticity constraints and in the spirit of FESR's they propose the following parametrization for the pp and p$\bar{p}$ cross sections:

$$\sigma_{tot} = 37.1(\frac{\nu}{m})^{-0.5}) + 37.2 - 1.44ln(\frac{\nu}{m}) + 90.2817ln^2(\frac{\nu}{m})$$

$$\sigma_{inel} = 62.59(\frac{\nu}{m})^{-0.5}) + 24.09 + 0.1604ln(\frac{\nu}{m}) + 0.1433ln^2(\frac{\nu}{m})$$

where ν denotes the lab energy, and at high energies $\nu = s/(2m)$.

W (Tev)	7	8	14	57
σ_{tot} mb	95.1 $\pm$ 1.1	97.6 $\pm$ 1.1	107.3 $\pm$ 1.2	134.8 $\pm$ 1.5
σ_{inel} mb	69.0 $\pm$ 1.3	70.3 $\pm$ 1.3	76.3 $\pm$ 1.4	92.9 $\pm$ 1.6

From Alan Martin's talk Trento Sept 2011 arXiv:1202.4966

and KMR Eur.Phys.J. C72(2012) 1937

	KMR model				KMR 3-ch eikonal				
energy	$\sigma_{\rm tot}$	$\sigma_{\rm el}$	$\sigma^{\rm SD}_{{\rm low}M}$	$\sigma^{\rm DD}_{{\rm low}M}$	$\sigma_{\rm tot}$	$\sigma_{\rm el}$	$B_{\rm el}$	$\sigma^{\rm SD}_{{\rm low}M}$	$\sigma^{\rm DD}_{{\rm low}M}$
1.8	72.7	16.6	4.8	0.4	79.3	17.9	18.0	5.9	0.7
7	87.9	21.8	6.1	0.6	97.4	23.8	20.3	7.3	0.9
14	96.5	24.7	7.8	0.8	107.5	27.2	21.6	8.1	1.1
100	122.3	33.5	9.0	1.3	138.8	38.1	25.8	10.4	1.6

Some results of the complete KMR model prior to the LHC data (left-hand Table), and results obtained from a simpler approach, based on a 3-channel eikonal description of all elastic (and quasi-elastic) pp and $p\bar{p}$ data, including the TOTEM LHC data (right-half of the Table). $\sigma_{\rm tot}$, $\sigma_{\rm el}$ and $\sigma^{\rm SD,DD}_{{\rm low}M}$ are the total, elastic and low-mass single and double dissociation cross sections (in mb) respectively. The cross section $\sigma^{\rm SD}$ is the sum of the dissociations of both the 'beam' and 'target' protons. $B_{\rm el}$ is the mean elastic slope (in GeV^{-2}), $d\sigma_{\rm el}/dt = e^{B_{\rm el}t}$, in the region $|t| < 0.2\ GeV^2$. The collider energies are given in TeV. The former (latter) analysis fit to the CERN-ISR observations that $\sigma^{\rm SD}_{{\rm low}M}$=2(3) mb at $\sqrt{s} = 53$ GeV, with low mass defined to be $M < 2.5(3)$ GeV.

Comparison of results obtained in GLM, Ostapchenko, K-P and KMR models

Ostapchenko (Phys.Rev.D81,114028(2010)) has made a comprehensive calculation in the framework of Reggeon Field Theory based on the resummation of both enhanced and semi-enhanced Pomeron diagrams.

To fit the total and diffractive cross sections he assumes TWO POMERONS: "SOFT POMERON" $\alpha^{Soft} = 1.14 + 0.14t$ "HARD POMERON" $\alpha^{Hard} = 1.31 + 0.085t$

The Durham Group (Khoze, Martin and Ryskin),(Eur.Phys.J.,C72(2012), 1937), in order to be consistent with the Totem result, have a new model, based on a 3-channel eikonal description, with 3 diffractive eigenstates of different sizes, but with ONLY ONE POMERON.

$$\Delta_{I\!P} = 0.14;\ \alpha'_{I\!P} = 0.1\ \ GeV^{-2}$$

Kaidalov-Poghosyan have a model which is based on Reggeon calculus, they attempt to describe data on soft diffraction taking into account all possible non-enhanced absorptive corrections to 3 Reggeon vertices and loop diagrams. It is a single $I\!P$ model and with secondary Regge poles, they have

$$\Delta_{I\!P} = 0.12;\ \alpha'_{I\!P} = 0.22 GeV^{-2}.$$

Comparison of results of various models

W = 1.8 TeV	GLM2	KMR2	Ostap	BMR*	KP	BH
$\sigma_{\rm tot}(mb)$	75.6	79.3	73.0	81.03		76.8
$\sigma_{\rm el}(mb)$	18.2	17.9	16.8	19.97		20.53
$\sigma_{SD}(mb)$	10.77	5.9(LM)	9.2	10.22	10.1	
$\sigma_{DD}(mb)$	5.93	0.7(LM)	5.2	7.67	5.8	
$B_{el}(GeV^{-2})$	17.6	18.0	17.8			16.8

W = 7 TeV	GLM2	KMR2	Ostap	BMR	KP	BH
$\sigma_{\rm tot}(mb)$	94.2	97.4	93.3	98.3		95.4
$\sigma_{\rm el}(mb)$	22.9	23.8	23.6	27.2		26.4
$\sigma_{SD}(mb)$	14.44	7.3(LM)	10.3	10.91	12.6	
$\sigma_{DD}(mb)$	7.15	0.9(LM)	6.5	8.82	6.0	
$B_{el}(GeV^{-2})$	19.8	20.3	19.0			18.3

W = 14 TeV	GLM2	KMR2	Ostap	BMR	KP	BH
$\sigma_{\rm tot}(mb)$	104.0	107.5	105.	109.5		107.3
$\sigma_{\rm el}(mb)$	26.1	27.2	28.2	32.1		31.0
$\sigma_{SD}(mb)$	16.78	8.1(LM)	11.0	11.26	14.0	
$\sigma_{DD}(mb)$	8.05	1.1(LM)	7.1	9.47	6.2	
$B_{el}(GeV^{-2})$	21.2	21.6	21.4			19.4

Conclusions

- Changes in parameter values between GLM1 and GLM2 are not dramatic, BUT three parameters m_1, γ and $G_{3\mathbb{P}}$ increase by 2-3 times in GLM2, driven by the LHC data.
- Increase of γ and $G_{3\mathbb{P}}$ is a direct consequence of the large diffractive cross-section measured at LHC.
- If the TOTEM results for σ_{tot} and σ_{el} are not amended, GLM will have to go back to the "drawing board".
- I don't believe that there is a "threshold" at W = 7 TeV, but the jury is still out.

GLM2 Differential cross section and Experimental Data at 1.8 and 7 TeV

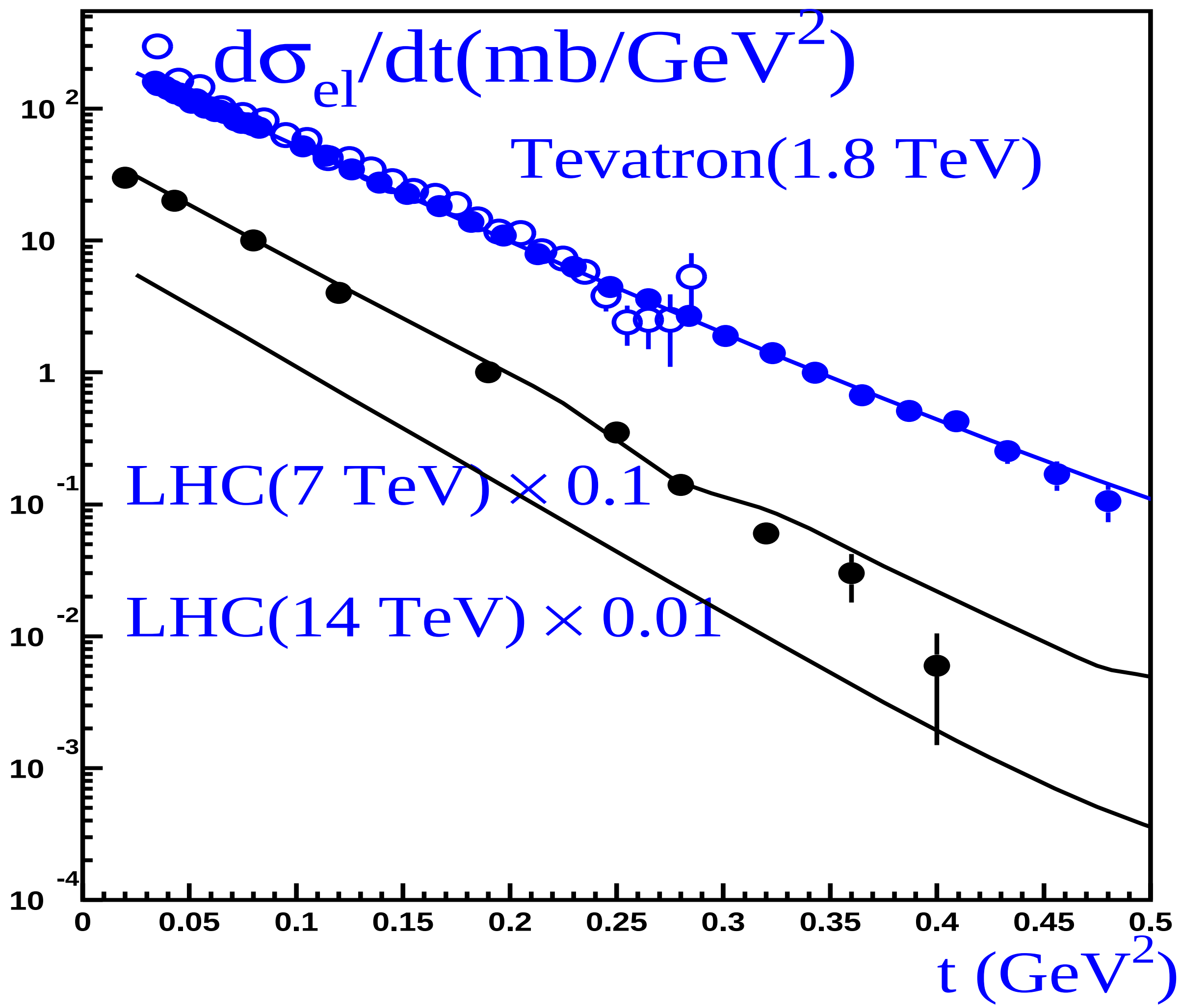

$d\sigma_{el}/dt$ versus $|t|$ at Tevatron (blue curve and data)) and LHC (black curve and data) energies ($W = 1.8\,TeV$ and $7\,TeV$ respectively) The solid line without data shows our prediction for $W = 14\,TeV$.

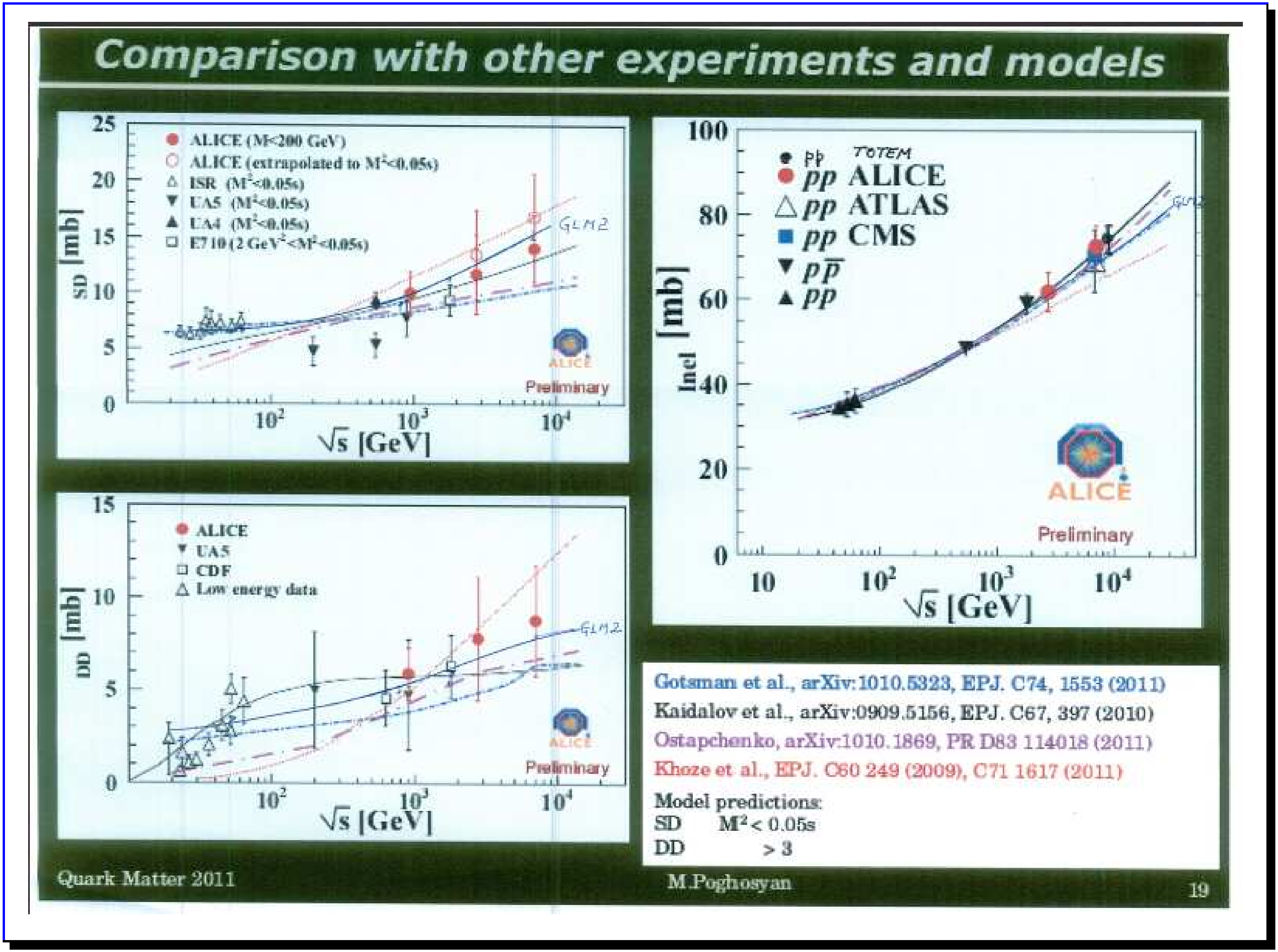
Comparison with other experiments and models
ALICE (M<200 GeV)
ALICE (extrapolated to M²<0.05s)
ISR (M²<0.05s)
UA5 (M²<0.05s)
UA4 (M²<0.05s)
E710 (2 GeV²<M²<0.05s)
GLM2
Preliminary
σSD [mb]
√s [GeV]
ALICE
UA5
CDF
Low energy data
σDD [mb]
pp TOTEM
pp ALICE
pp ATLAS
pp CMS
pp̄
pp
σinel [mb]
Gotsman et al., arXiv:1010.5323, EPJ. C74, 1553 (2011)
Kaidalov et al., arXiv:0909.5156, EPJ. C67, 397 (2010)
Ostapchenko, arXiv:1010.1869, PR D83 114018 (2011)
Khoze et al., EPJ. C60 249 (2009), C71 1617 (2011)
Model predictions:
SD M² < 0.05s
DD > 3
Quark Matter 2011
M.Poghosyan
19

Guiding criteria for GLM Model

- The model should be built using Pomerons and Reggeons.
- The intercept of the Pomeron should be relatively large. In AdS/CFT correspondence we expect $\Delta_{I\!P} = \alpha_{I\!P}(0) - 1 = 1 - 2/\sqrt{\lambda} \approx$ 0.11 to 0.33. The estimate for λ from the cross section for multiparticle production as well as from DIS at HERA is $\lambda\ =$ 5 to 9;
- $\alpha'_{I\!P}(0)\ =\ 0$;
- A large Good-Walker component is expected, as in the AdS/CFT approach the main contribution to shadowing corrections comes from elastic scattering and diffractive production.
- The Pomeron self-interaction should be small (of the order of $2/\sqrt{\lambda}$ in AdS/CFT correspondence), and much smaller than the vertex of interaction of the Pomeron with a hadron, which is of the order of λ;

Diffraction

For double diffraction we have (see Fig.1b):

$$A^{dd}_{i,k} \;=\; \int d^2b'\, 4\, g_i\left(\vec{b}-\vec{b}', m_i\right)\; g g_k\left(\vec{b}', m_k\right)$$
$$\times\;\; Q\left(g_i, m_i, \vec{b}-\vec{b}', Y-Y_1\right)\, e^{2\Delta\,\delta Y}\, Q\left(g_k, m_k, \vec{b}', Y_1-\delta Y\right).$$

This equation is illustrated in fig-b, which displays all ingredients of the equation. We express each of two cut Pomerons through the Pomeron without a cut, using the AGK cutting rules. For single diffraction, $Y = \ln\left(M^2/s_0\right)$, where, M is the SD mass. For double diffraction, $Y - Y_1 = \ln\left(M_1^2/s_0\right)$ and $Y_1 - \delta Y = \ln\left(M_2^2/s_0\right)$, where M_1 and M_2 are the masses of two bunches of hadrons produced in double diffraction.

The integrated cross section of the SD channel is written as a sum of two terms: the GW term, which is equal to

$$\sigma^{GW}_{sd} \;=\; \int\; d^2b\left|\alpha\beta\{-\alpha^2\, A_{1,1} + (\alpha^2-\beta^2)\, A_{1,2} + \beta^2\, A_{2,2}\}\,\right|^2.$$

Diffraction 2

The second term describes diffraction production due to non GW mechanism:

$$\sigma_{sd}^{\mathrm{nGW}} \;=\; 2\int dY_m \int d^2b \tag{1}$$

$$\Big\{ \alpha^6\, A^{sd}_{1;1,1}\, e^{-\Omega_{1,1}(Y;b)} \;+\; \alpha^2\beta^4 A^{sd}_{1;2,2}\, e^{-\Omega_{1,2}(Y;b)} + 2\,\alpha^4\,\beta^2\, A^{sd}_{1;1,2}\, e^{-\frac{1}{2}\left(\Omega_{1,1}(Y;b)+\Omega_{1,2}(Y;b)\right)}$$

$$+\;\beta^2\,\alpha^4\, A^{sd}_{2;1,1}\, e^{-\Omega_{1,2}(Y;b)} \;+\; 2\,\beta^4\alpha^2\, A^{sd}_{2;1,2}\, e^{-\frac{1}{2}\left(\Omega_{1,2}(Y;b)+\Omega_{2,2}(Y;b)\right)} \;+\; \beta^6\; A^{sd}_{2;2,2}\, e^{-\Omega_{2,2}(Y;b)} \Big\}.$$

The cross section of the double diffractive production is also a sum of the GW contribution,

$$\sigma_{dd}^{GW} \;=\; \int\; d^2b\;\alpha^2\,\beta^2 \Big| A_{1,1} \;-\; 2\,A_{1,2} \;+\; A_{2,2} \Big|^2,$$

to which we add the term which is determined by the non GW contribution,

$$\sigma_{dd}^{\mathrm{nGW}} \;=\; \int\; d^2b\;\Big\{ \alpha^4\, A^{dd}_{1,1}\, e^{-\Omega_{1,1}(Y;b)} \;+\; 2\alpha^2\,\beta^2 A^{dd}_{1,2}\, e^{-\Omega_{1,2}(Y;b)} \;+\; \beta^4\, A^{dd}_{2,2}\, e^{-\Omega_{2,2}(Y;b)} \Big\}.$$

In our model the GW sector can contribute to both low and high diffracted mass, as we do not know the value of the typical mass for this mechanism, on the other hand, the non GW sector contributes only to high mass diffraction ($M_0^{nGW} \;\geq$ 20 GeV).

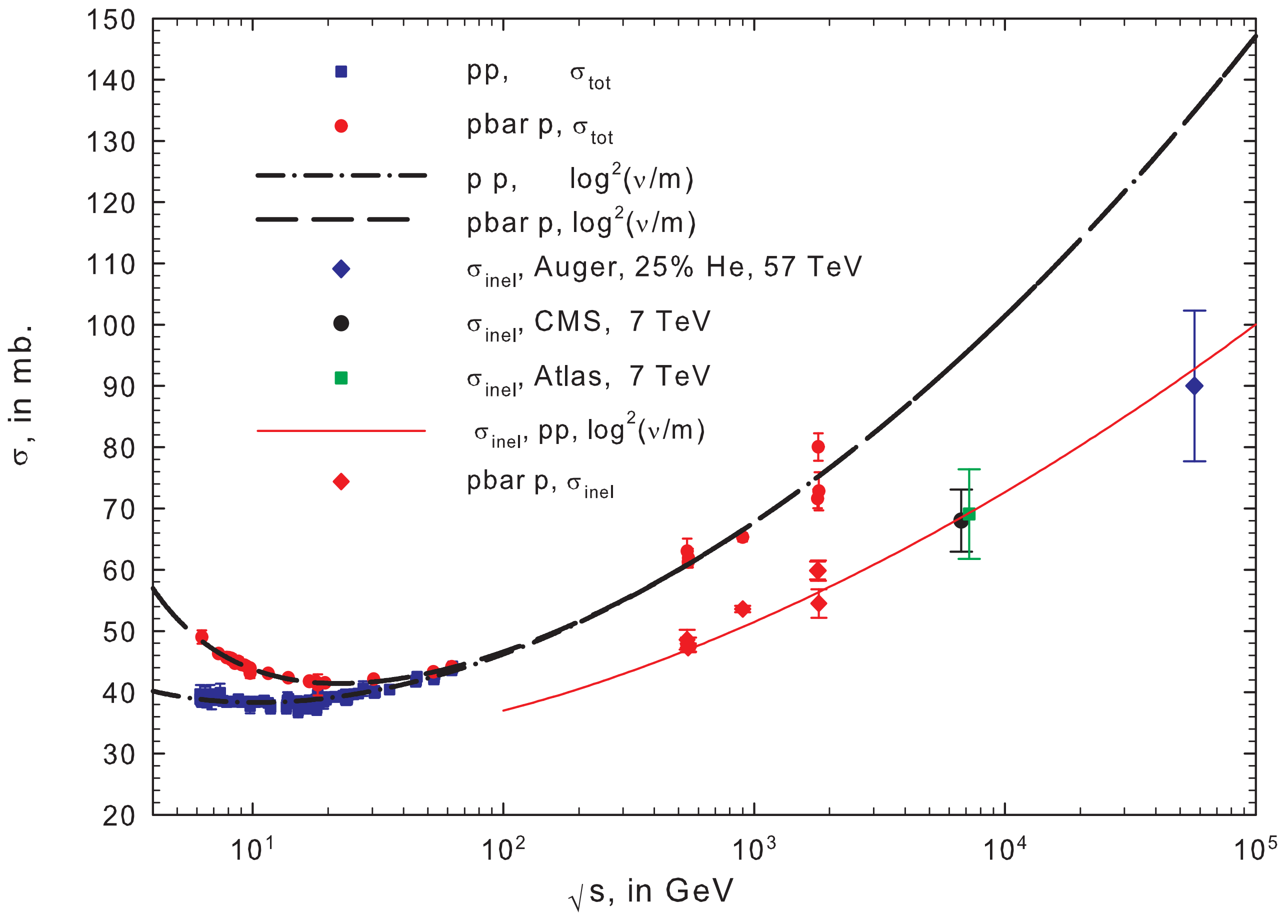
150
140
130
120
110
100
90
80
70
60
50
40
30
20
σ, in mb.
pp, σ tot
pbar p, σ tot
p p, log2(ν/m)
pbar p, log2(ν/m)
σ inel, Auger, 25% He, 57 TeV
σ inel, CMS, 7 TeV
σ inel, Atlas, 7 TeV
σ inel, pp, log2(ν/m)
pbar p, σ inel
10^1
10^2
10^3
10^4
10^5
√s, in GeV